Article

Development of Lumped Parameter Model for an Aeronautic Hybrid-Electric Propulsion System

E. Frosina [1,*], A. Senatore [1,†], L. Palumbo [1,†], G. Di Lorenzo [2,†], C. Pascarella [2,†]

[1] University of Naples "Federico II", Via Claudio, 21 – 80125 – Naples, Italy; Emma Frosina <emma.frosina@unina.it>, Adolfo Senatore <senatore@unina.it>, Luca Palumbo <luca.palumbo92@icloud.com>.

[2] Centro Italiano Ricerca Aerospaziale, Via Maiorise – 81043, Capua (CE), Italy, Di Lorenzo Giuseppe <G.DiLorenzo@cira.it>, Ciro Pascarella <C.Pascarella@cira.it>

* Correspondence: emma.frosina@unina.it; Tel.: +39-081-768-32-76

† These authors contributed equally to this work.

Abstract: This paper describes a case study for applying of hybrid-electric propulsion system for a general aviation aircraft. The work was performed by a joint team of CIRA and the Department of Industrial Engineering of the University of Naples "Federico II". Electric and hybrid electric propulsion for aircraft has gained widespread and significant attention over the past decade. The driver for industry interest has principally been the need to reduce emissions of combustion engine exhaust products and noise, but increasingly studies revealed potential for overall improvement in energy efficiency and mission flexibility of new aircraft types. The project goal was to demonstrate feasibility of aeronautic parallel hybrid-electric propulsion for a Light aircraft varying the mission profiles and the electric configuration. Through a creation, and application, of a global model, with software AMESim®, in which it can be represented everything about the components chosen by the industrial partners, some interesting considerations are carried out.

In particular, it was confirmed that with the only integration of state of the art technologies, for some particular missions, the advantages of aircraft hybrid-electric propulsion, for light aircraft, are notable.

Keywords: lumped parameter simulation; aircraft hybrid propulsion; fuel fconomy; propulsion and propellant systems.

1. Introduction

The aviation industry is responsible for 12% of the total transportation impact of CO_2 while awareness, for decreasing the total carbon footprint, is rising. Both the aerospace and the automotive industry are facing an increasing pressure from society to make the transportation sector more sustainable. Within the automotive industry slowly an increase in electric vehicles can be noticed (<1%). Also in the aerospace industry, a rise in electrification can be seen, with small aircraft as the E-Star and E-Fan [1] (two seaters) as commercial examples. Electrification of the transportation sector could further result in a decrease in noise and an increase in lifespan of parts as vibrations are decreased.

This research is focused on the study of aeronautical hybrid-electric propulsion to analyze the consumption and emissions saving compared to a benchmark ICE. The request of greener propulsive systems for a/c is dictated by near future target in terms of air pollution and noise. Currently, aviation is responsible of a considerable part of CO_2 introduced in the atmosphere with

Peer-reviewed version available at Aerospace 2018, 5, 105; doi:10.3390/aerospace5040105

about 12% as clear reported by National Geographic on 2015 [2]. The aircrafts emitted about 700 million tons of the CO_2, during the 2013. [2] estimated that, without any changes, this number will be tripled by 2050. Another interesting study has been carried out by the British Airways [3]. The local quality of air near airports presents a high concentration of NO_x and CO, this concentration is regulated by the UE Directive. The aircrafts electrification would represent the best option to reach the ideal "clean" and high efficiency mobility. For this reason, during the recent years, the electric traction has been applied to achieve noise and emission reductions. The electrical technology has developed new systems to improve the velocity and autonomy, however, the electrification of aircrafts has many obstacles due essentially to the battery pack and them density of energy. The target of many studies is focused on the buildup of the specific density of the batteries to support the modern electric machines for a greater endurance in the time.

Hence, the full replacement of the fossil fuel with green energies is impossible in the near future and, consequently, different technological solutions to reduce the environment impact due to emissions must be applied. For this reason, the European Union has established a program called Clean Sky which is the largest European research program to develop innovative cutting-edge technology aimed on the reduction the environmental and noise emissions due to the aeronautic vehicles.

On this scenario, the hybrid propulsion technology represents a great solution for the near future. Hybridization consists of a mechanical coupling, in series or in parallel, of an internal combustion engine with an electric machine connected to a battery system; where the ICE is the principal powering engine. The use of two different type of propulsions allows to benefit of the advantages and to compensate eventually issues of each engine. In this way, the power-unit get a higher efficiency. The hybrid propulsion systems are claiming themselves in the transportation sector with a great success by exploiting the best of the thermal power with the integration of electrical power causes a consequently reduction the total pollution. This reduction, however must be maximize if compared with the normal propulsion system.

It is known that the specific energy of liquid fossil fuel is fifty times more than batteries. Therefore, in the study of a hybrid architecture this aspect must be considered.

M. Cui et al. [4] have modelled, simulated and optimized the operation of an aeronautic hybrid-electric system close to our project. The electric machine is located on the same shaft of the internal combustion engine; therefore, both rotate at the same speed. Then the shaft is connected to the propeller. In the 2012, Joseph K. Ausserer and Frederick G. Harmon [5] have simulated and prototyped a hybrid-electric system for a small airplane remotely piloted. The little airplane is powered by the ICE of Honda GX 35 (of 35 cm^3), with a power of 0.97 kW at 7000 rpm and the electric motor AXI 4130/20, with a power of 0.64 kW, powered by the battery 6xTP3300-4S (Lithium polymer, 0.248 kWh). In the 2014, C. Friedrich e P.A. Robertson [6] have also simulated and prototyped a hybrid-electric system for an ultra-light aircraft. The plane is the SONG, developed by Gramex Ltd, usually equipped with a Bailey V5 (of 200 cm^3) capable of delivering up to 15 kW. The Bailey engine has been replaced with the Honda GX160 (of 7,5 kW at 7000 rpm in 12 kg) connected with a DC brushless JM1 of the Joby Motors (of 12 kW in 2,8 kg), able to work also as generator to recharge the battery.

This paper is focused on the hybridization of an ultra-light aircraft the "Tecnam P2010" [7]. The Tecnam P2010 is usually equipped with the engine IO-360-M1A (powered by AVGas 100LL), built up by AVCO Lycoming [8]. The engine has four opposing cylinders, air cooled, with a maximum power of 130 kW and a displacement is of 5900 cm^3. The total weight when installed on the ultra-light aircraft is of 190 kg. The Tecnam P2010 has been completely modified in the hybridization process, replacing the Lycoming engine with CMD 22 that has a reduced weight and size and adding an electrical machine, which can also function as generator, and a battery pack [9-10]. The CMD 22, has four cylinders in a boxer configuration with a displacement of 2200 cm^3, a maximum power of 102 kW and a total weight is 82 kg [11].

The sizing and the choice of each component has been done using a numerical approach with the commercial code AMESim®, developed by Siemens®. Then the model results have been compared

Preprints (www.preprints.org) | NOT PEER-REVIEWED | Posted: 30 June 2018 doi:10.20944/preprints201806.0499.v1

Peer-reviewed version available at *Aerospace* **2018**, *5*, 105; doi:10.3390/aerospace5040105

with the performance of the baseline configuration. For this reason, a model of the baseline propulsion system has been also built up. The simulations highlight a fuel saving over the 12% for the training profile and amount the 6% for the cruise profile.

2. The hybrid-electric propulsion system description

Since the aim of the research is to demonstrate the feasibility of hybrid electric propulsion for an ultra-light aircraft the study has been conducted on an aircraft already available on the market and powered by a conventional internal combustion engine. The research carried out shows that a hybrid-electric solution is optimal for this aircrafts category to reduce both emissions and fuel consumption.

The analyzed ultra-light aircraft is, as said in the introduction, the Tecnam P2010 that is usually equipped with the IO-360-M1A (powered by AVGas 100LL), built up by AVCO Lycoming. The IO-360-M1A has four opposing cylinders, air cooled with a maximum power of 130 kW and a displacement is of 5900 cm3. The total weight is of 135 kg while when installed the weight becomes of 190 kg. Therefore, the hybrid-electric motor must have the same power and the same weight to be proposed as alternative to the ICE.

The hybridization of the engine consists on the introduction of a smaller ICE combined with an electric machine an inverter and a battery pack

2.1. The hybrid-electric configuration, system propulsion scheme and hybridization grade

A parallel hybrid-electric architecture has been chosen after an accurate analysis of the various configuration alternative. With a parallel architecture the internal combustion engine is chosen to ensure the power required for cruise, while the electric motor intervenes at the stage where maximum power is required (take-off and climb). The internal combustion engine, in this way, can operate at minimum specific consumption (maximum efficiency) during the cruise, using the electric machine as generator to recharge the battery pack. The layout of the chosen architecture is presented in figure 1.

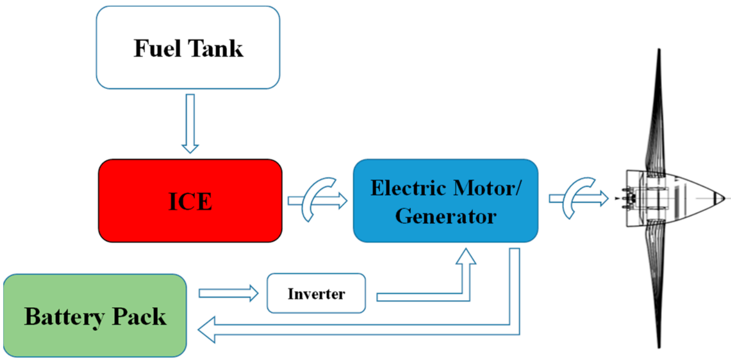

Figure 1. Layout of hybrid propulsion system.

As shown in figure 1, the electric motor/generator and the internal combustion engine are linked to the same shaft, working at the same speed. The rotating speed of both motors is reduced with ratio of 2:1 before the propeller. This configuration allows a remarkable saving of weight, because both motors are located in a one single block.

Each component of the system has been accurately chosen considering that the hybrid-electric solution must cover the aircraft requests and replace the original propulsion, the Lycoming IO-360-M1A.

The internal combustion engine chosen in this research is the CMD 22, manufactured by and Italian company CMD-engine. The CMD 22 is a positive ignition engine for ultra-light aircraft (Maximum Take-Off Mass of 1200 kg), powered by an automotive fuel with four cylinders in boxer configuration; the displacement is of 2200 cm^3 while the maximum power is of 102 kW. The total weight is of only 82 kg.

The injection system (direct injection) is made by two electric injectors, placed on the aspiration manifold of each cylinder, and by two ignition candles. Cylinders are opposite horizontally, closed in one block in which the camshaft manages the four intake and exhausts valves for each cylinder. In figure 2, the main features of the CMD 22 are listed.

Architecture	4 Cylinder Box
Bore	100 [mm]
Stroke	70 [mm]
Displacement	2200 [cm³]
Compression Ratio	10.5
Naturally Aspirated	
Valves\Cylinder	4
Fuel Injection System	Indirect Electronic Injection System Multi Point
Fuel	Gasoline
EECS	SINGLE FADEC EDU
Alternator	14 [V]
Cooling System	Air/Oli
Dry Weight	82 [kg] - with Gearbox
Dimension L*W*H	638*328*372 [mm] - with Gearbox
Take Off Power	90 [kW] - At the Propeller Shaft (122 Hp)
Continuous Power	74 [kW] - At the Propeller Shaft
Min. BSFC	285 [g/kWh] - At the Propeller Shaft

Figure 2. Features of the internal combustion engine: CMD22.

Since the propeller must work at 2700 rpm, both engines will run at about 5500 rpm. At this rotation speed the internal combustion engine CMD 22 gives 90 kW while the other 35 kW comes from the electric, replacing the performance of the original propulsion.
Another important aspect is, as said, the overall weight of the entire system that must be below the 135 kg, weight of the Lycoming IO-360-M1A engine. For this reason, since the engine CMD 22 has a weight of 82 kg, the total weight of the electric machine, the battery and the control systems have to be of about 65 kg.

Today, there are in production some ultra-light motors with the kW/kg ratio equal to 5. In any way, considering a little motor of 6-8 kg the control systems and the auxiliaries, the maximum weight for the battery pack is of 55 kg.

The total weight of the aircraft can be reduced of about 15 kg by using the electric machine also as starter motor. Another important aspect that must be considered in the choice of the EM is its capacity to run under several operative conditions, as indicated in the table 1.

Table 1. Starter torque in function of different temperature conditions

Temperature [°C]	Starting Torque [Nm]
-10	216
-20	523
-25	761
-30	1047
-40	1593

EMs for the aeronautical application must respect many other peculiarities. There are in literature examples of a full-electric aircraft [12-13] where it has been demonstrated the real applicability of HTS (High Temperature Superconducting). HTS motors have, in fact, high density of power and lower dimension respect to the traditional motors. On the other hand, it is requested, for these electric machines, to work at low temperature (of about 50 K), to operate at the best performance. Therefore, their application requests an efficient cooling system. Despite the cooling system, the motor has been installed with a cryocooler of 60 kg, but in general the weight has been reduced. The cryocooler can produce cryogenic gas able to maintain the superconductor temperature low. This weight saving can be used to grow up the aircraft's autonomy with many batteries.

Preprints (www.preprints.org) | NOT PEER-REVIEWED | Posted: 30 June 2018 doi:10.20944/preprints201806.0499.v1

Peer-reviewed version available at *Aerospace* **2018**, *5*, 105; doi:10.3390/aerospace5040105

There are available on the market many motors that fit with our project. The final choice is the EMRAX 208 [10] manufactured by ENSTROJ. This EM is an axial flux synchronous permanent magnet motor/generator, sinusoidal three phases motor.

Main features of the EMRAX 208 motor are listed in table 2.

Table 2. Technical data - EMRAX 208

Technical data - EMRAX 208 High Voltage	
Air cooled	AC
Air Flow = AF, Ambient Air = AA	AF=20m/s; AA=25°C
Weight	9,1 [kg]
Diameter ø / width	208 / 85 [mm]
Maximal battery voltage and full load/no load RPM	470 [Vdc] (5170/7050 RPM)
Peak motor power at max RPM	80 [kW]
Continuous motor power	20 – 32 (at 3000-5000 RPM)
Maximal rotation speed	6000 (7000 peak) [RPM]
Maximal motor current	200 [Arms]
Continuous motor current	100 [Arms]
Maximal peak motor torque	150 [Nm]
Continuous motor torque	80 [Nm]
Motor efficiency	92-98%
Internal phase resistance at 25 °C	12,0 [mΩ]
Wire connection star Induction Ld/Lq	125/130 [μH]
Controller / motor signal	sine wave
AC voltage between two phases	0,0487 [Vrms/1RPM]
Magnetic flux – axial	0,0393 [Vs]
Number of pole pairs	10
Rotor Inertia (d=160mm; m=4,0kg)	256 [kg*cm²]

The hybridization factor (HF) of the hybrid-electric propulsion under investigation has been defined after the choice of the ICE and the EM. As know, there are three categories of hybridization:

- Full Hybrid (also called full hybridization): the electric system is able to move the aircraft by itself on a normalized guide cycle, without the battery support ($HF > 0.38$),
- Mild Hybrid (also called light hybridization): the full-electric is not able to follow all the guide cycles ($0.23<HF<0.38$),
- Minimal Hybrid: lower distance done in pure electrical mode ($HF<0.23$).

The HF is obtained by the following expression:

$$HF = \frac{P_{EM}}{P_{ICE} + P_{EM}} = \frac{P_{EM}}{P_{TOT}} \tag{1}$$

Where P_{EM} is the power coming from the electrical system and P_{ICE} is the rate from the internal combustion system. The HF follows in the range [0 ÷ 1] where respectively zero indicates a conventional endothermic vehicle and one is a full-electric vehicle. In our case, the HF assumes a value of 0.26 because 32 kW of power comes for the electric motor and 90 kW from the internal combustion engine. For this reason, the system falls in the light hybridization category since the electric motor cannot operate alone at any stage of a normalized cycle.

The main components of the proposed hybrid-electric propulsion system have been selected mainly for their performance and weight. In the next paragraph, a numerical model of the entire propulsion system is described. The model has been built up using the lumped parameter code

Preprints (www.preprints.org) | NOT PEER-REVIEWED | Posted: 30 June 2018 doi:10.20944/preprints201806.0499.v1

Peer-reviewed version available at Aerospace 2018, 5, 105; doi:10.3390/aerospace5040105

AMESim LMS® (developed by Simerics®) [14]. The numerical model has been then used for predicting the performance of the overall system to allow the assessment and the validation of the control strategies. Each part of the propulsion has been included in the model divided in: mechanical elements, signals, propeller, mission profiles, EM and ICE.

3. Lumped parameter model/ Model assumption

The structure of the lumped parameter numerical model used for the simulation of the hybrid-electric propulsion system is shown in figure 3. The hybrid propulsion of the ultra-light aircraft has been modelled splitting the system in five units:

- The internal combustion engine,
- The electrical components. This sub-model includes the electrical machine.
- The cooling system,
- The propeller
- Mission profiles.

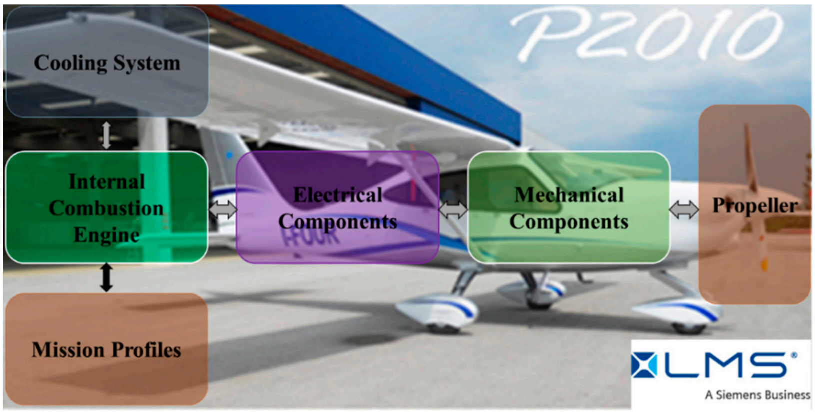

Figure 3. Structure of the lumped parameter model of the Hybrid-Electric Propulsion System.

Each unit, of figure 3, has been modelled using the commercial code AMESim® developed by Siemens®. The entire model of the hybrid-electrical propulsion system is shown in figure 4.

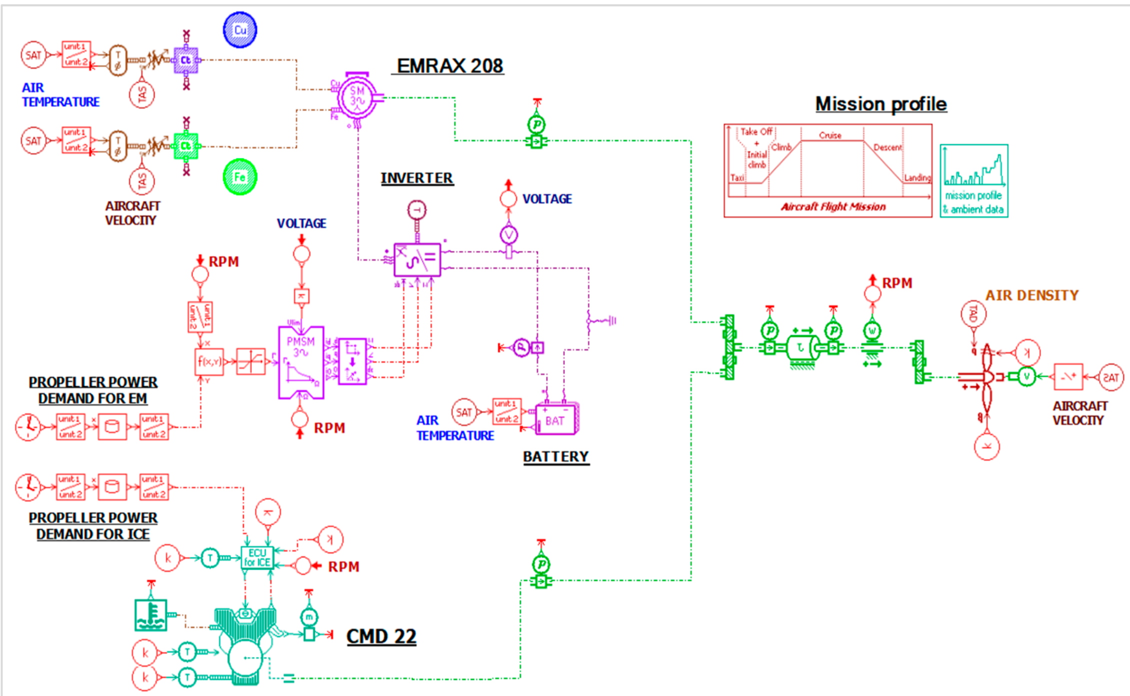

Figure 4. The complete model of the Hybrid-Electrical propulsion system.

Peer-reviewed version available at *Aerospace* **2018**, *5*, 105; doi:10.3390/aerospace5040105

Form figure 4, the five sub-systems of the entire propulsion unit are clearly shown. Before running simulation, the input parameters to the numerical model have been defined. Two important parameters are the mission profiles (training and cruse) and the flight speed.

The main goal of the modeling task is to build a tool able to estimate performances of the hybrid system for each mission profile. Mission profiles and the flight speed assigned are described by following in this paragraph.

3.1 Training profile

As said, before describing the model result, the input to the model must be defined. Input are the mission profiles and the flight speed of the aircraft. The "training" is one of the mission profiles analyzed in this paper. It is composed by segments repeated more times. In fact, excluding take-off and the taxi segments that happen just one time, the others are repeated interspersed with "touch and go" phases for climbing again. For this reason, this mission profile is also called "touch and go" profile. The training profile is clearly shown in figure 5.

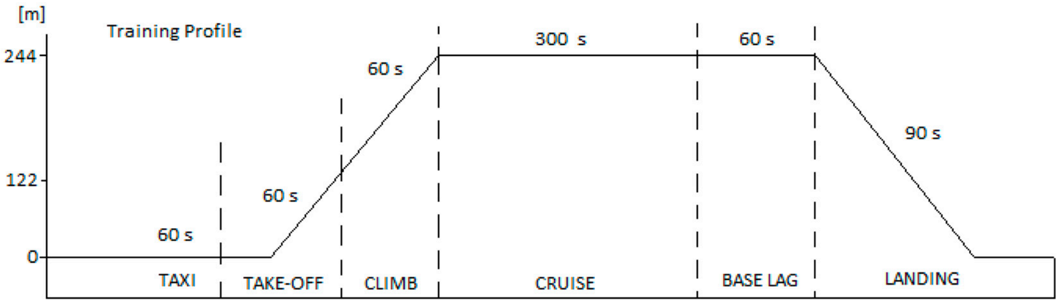

Figure 5. Training Profile.

Depending on the battery energy storage capability, the aircraft can do several "touch and go" as show in the table 3.

Table 3. Training Profile

Phase	Time [s]	Altitude [m]	Power at propeller [kW]
Take-off	60	122	122 (90 ICE + 32 EM)
Climb	60	244	103 (80 ICE + 23 EM)
Cruise	300	244	68 (60 ICE + 8 EM)
Base leg	60	244	23 (35 ICE – 12 GEN)
Landing	90	0	23 (35 ICE – 12 GEN)

In the table 3, the power available at the propeller has been split in the contribution of the internal combustion engine and of the electric machine. During the take-off both motors must work at the maximum power with consequently less power from the EM during the climb and a little bit during the cruise (with just 8 kW). Only during the base leg and the landing phases, the internal combustion engine is the one drives the propeller; part of the ICE power goes also to recharge the battery. As said, the internal combustion engine gives 35 kW this means that, during the base leg and the landing were only 23 kW are requested, the other 12 kW goes to the generator (1/3 of its maximum power).

The last parameter requested for the simulation is the flight velocity during the training mission profile. Speed values for each phase of the mission profile are listed in table 4. These data have been given by company Tecnam, the manufacturer of the aircraft under investigation.

Preprints (www.preprints.org) | NOT PEER-REVIEWED | Posted: 30 June 2018 doi:10.20944/preprints201806.0499.v1

Peer-reviewed version available at Aerospace 2018, 5, 105; doi:10.3390/aerospace5040105

Table 4: Flight velocity during the training profile

Phase	V_0
Take-Off	45(m/s) = 88 knots
Climb	41.15(m/s) = 80 knots
Cruise	61.7(m/s) = 120 knots
Base Lag	31(m/s) = 60 knots
Landing	36(m/s) = 70 knots

3.2 Cruise Profile

The cruise profile is completely different from the training. In fact, there is a single cycle during which the maximum power has to be guaranteed from the internal combustion engine for all the cruise phase and a minimum recovery goes to the electric machine that works like generator.

Table 5 Cruise Profile

Phase	Time [s]	Altitude [m]	Power at propeller [kW]
Take-off	60	122	122 (90 ICE + 32 EM)
Climb	720	2440	93 (70 ICE + 23 EM)
Cruise	8400	2440	88.5 (90 ICE – 1.5 EM)
Base leg	720	0	23 (25 ICE – 2 GEN)
Landing	60	122	122 (90 ICE + 32 EM)

The cruise profile, as shown in both table 5 and figure 6, consists of four segments. The first one is the take-off that last 60 s, then the climb with 720 s and the main part the cruise segment (8400 s). By the end, the landing (duration of 720s); therefore, for this profile, there are no touch and go as for the training profile.

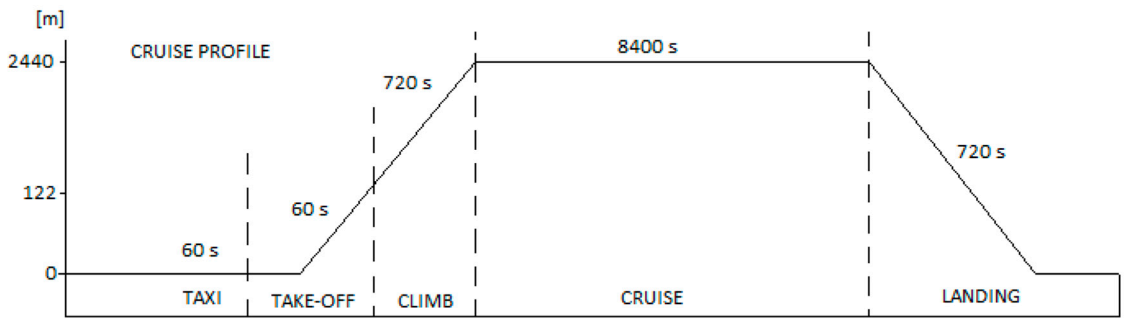

Figure 6. Cruise Profile.

As done for the training profile, also for the cruise the flight speed need to be insert as input to the numerical model. Data have been supplied by company Tecnam, [7] the manufacturer of the aircraft. During the take-off segment the aircraft has a speed of 88 knots, then, during the climb the speed is of 88 knots and becomes 120 knots in the Cruise segment. Landing, the last phase, last 70 s at 70 knots.

Table 6. Flight velocity during the cruise profile

Phase	V_0
Take-Off	45(m/s) = 88 knots
Climb	41.15(m/s) = 80 knots
Cruise	61.7(m/s) = 120 knots
Base Lag	31(m/s) = 60 knots
Landing	36(m/s) = 70 knots

Peer-reviewed version available at *Aerospace* **2018**, *5*, 105; doi:10.3390/aerospace5040105

As said, the entire numerical model of the propulsion includes five sub-parts. One of them concerns the electrical part where the battery is one of the main components. Therefore, before running simulation an accurate study has been performed to choose the best battery pack for the specific application.

3.3 Battery

The choice of the battery pack is crucial in this project because it has to satisfy several requirements imposed by the mission profiles already described. However, there are other two important aspects to consider: the weight and volume limits [15-16].

The battery must be able to deliver current (at a specific intensity and voltage) to the electric motor for giving the power required. Therefore, the choice of cells number does not depend only on the weight but also on the current that can be delivered and on the reduction of the voltage. Several typologies of cells available on the market, and for this project the lithium-polymer has been chosen for the great specific energy. A great specific energy means that, with the same energy required, these batteries have minor mass. As said the battery pack would be able to guarantee two different mission profiles (training and cruise). Where, the energy that the battery has to storage for only one training profile is of 1.58 kWh while for the cruise profile is of 5.13 kWh.

The battery capacity for the training profile, has been defined considering the maximum voltage that the electric motor can accept by the battery, namely 500V. Therefore, it assumes the value of almost 16 Ah.

The final choice for the battery pack were the Superior Lithium Polymer Battery SLPB78205130H of KOKAM, South Korea's leading manufacturer of lithium-polymer.

The feature of the Kokam battery cells are listed in table 7.

Table 7: Summary table of battery chosen

Items	Specification			Remarks
Rated Capacity	16 Ah			Charge @0,2C, 23 3 °C Discharge@0,2C, 23±3 °C
Energy Density	Gravity		146 Wh/kg	
	Volume		359 Wh/l	Excluded tab and seal
Internal Resistance	Max. 1,1 mW			AC @ 1kHz
Weight	Max. 406g			
Cell Dimension [Maximum]	Width		217 mm	Unfolded
	Length		137 mm	Excluded tab length
	Thickness		7,5 mm	3,7 ± 0,1V
Voltage	Average		3,7 V	
	Lower Limited		2,7 V	
	Upper Limited		4,2 V	
Current [Maximum]	Charge	Cont.	48,0 A (3C)	23±3 °C
	Discharge	Cont.	128,0 A (8C)	23±3 °C
		Peak	240,0 A (15C)	< 10s, > SOC 50%
Cycle Life to 80% of Remaining Capacity	1C/1C		1,4	100% DOD or 3,0~4,2 V (@23±3 °C)

Kokam battery cells have weight is of 0.406 g with a density of energy of 146 Wh/kg; therefore, to reach the 8 kWh requested by the electrical motor, the final weight is of 55 kg. This confirms that both the 5 cycles of the training and the cruise profile could be possible with this battery pack.

The model of the battery pack is shown in figure 7.

All the inputs to the numerical model have been implemented as the number, the disposition and the capacity of the cells, resistance and the open circuit voltage as function of the state of charge. The resistance and the open circuit voltage, as function of the state of charge, have been valued including the discharge curves in figure 7b). Those trends have been plotted as function variation of C-rate. In the numerical model the battery pack's input (shown in figure 8a) have been obtained for

Preprints (www.preprints.org) | NOT PEER-REVIEWED | Posted: 30 June 2018 doi:10.20944/preprints201806.0499.v1

Peer-reviewed version available at *Aerospace* **2018**, *5*, 105; doi:10.3390/aerospace5040105

the datasheet of the chosen battery pack. The numerical model, as output, evaluates the OCV (Open Circuit Voltage) and the resistance at 25 C° for the variation of state of charge, figure 8a). All the evaluated information are enough to calculate the true state of charge during the simulation, the variation of current and voltage and the apparent power guaranteed.

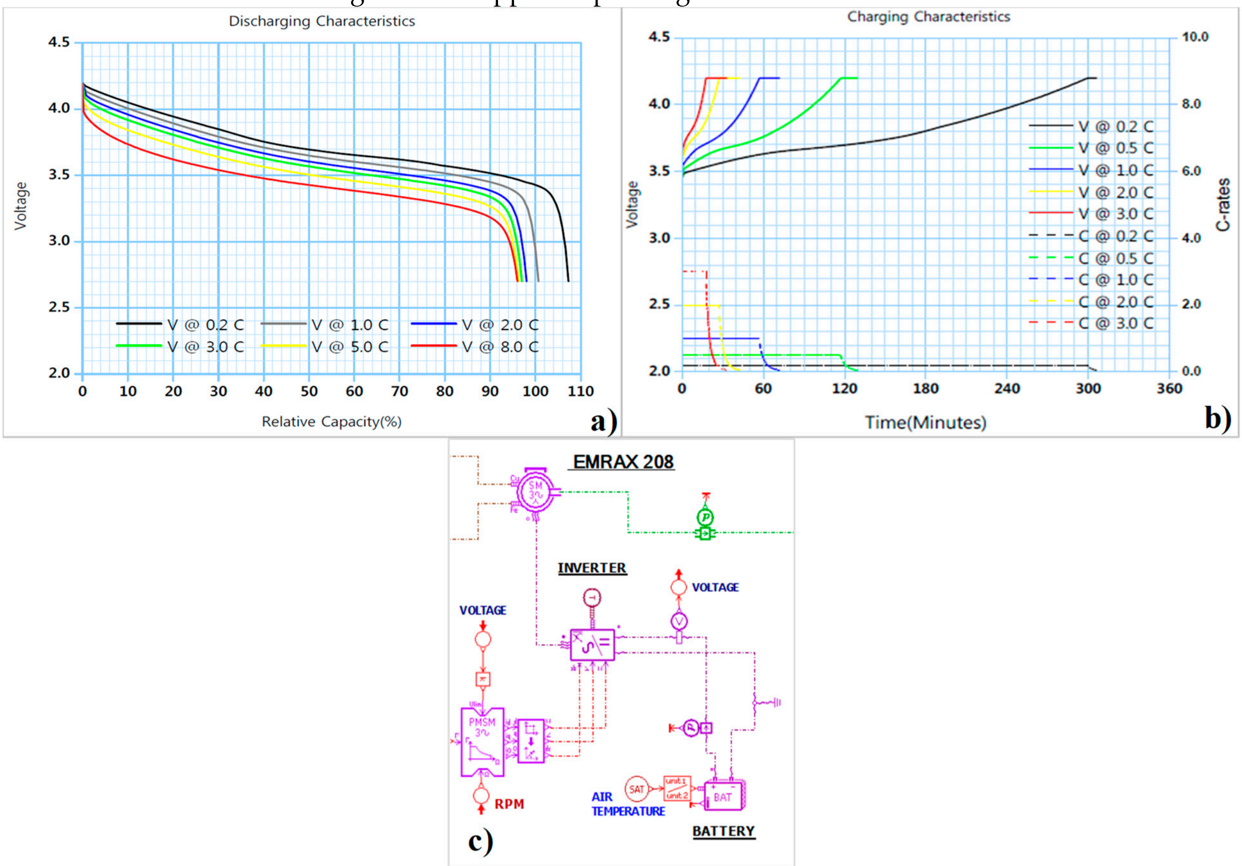

Figure 7. a) Discharging characteristics of the kokam 16Ah, b) Charging characteristics of the kokam 16Ah, c) Numerical model.

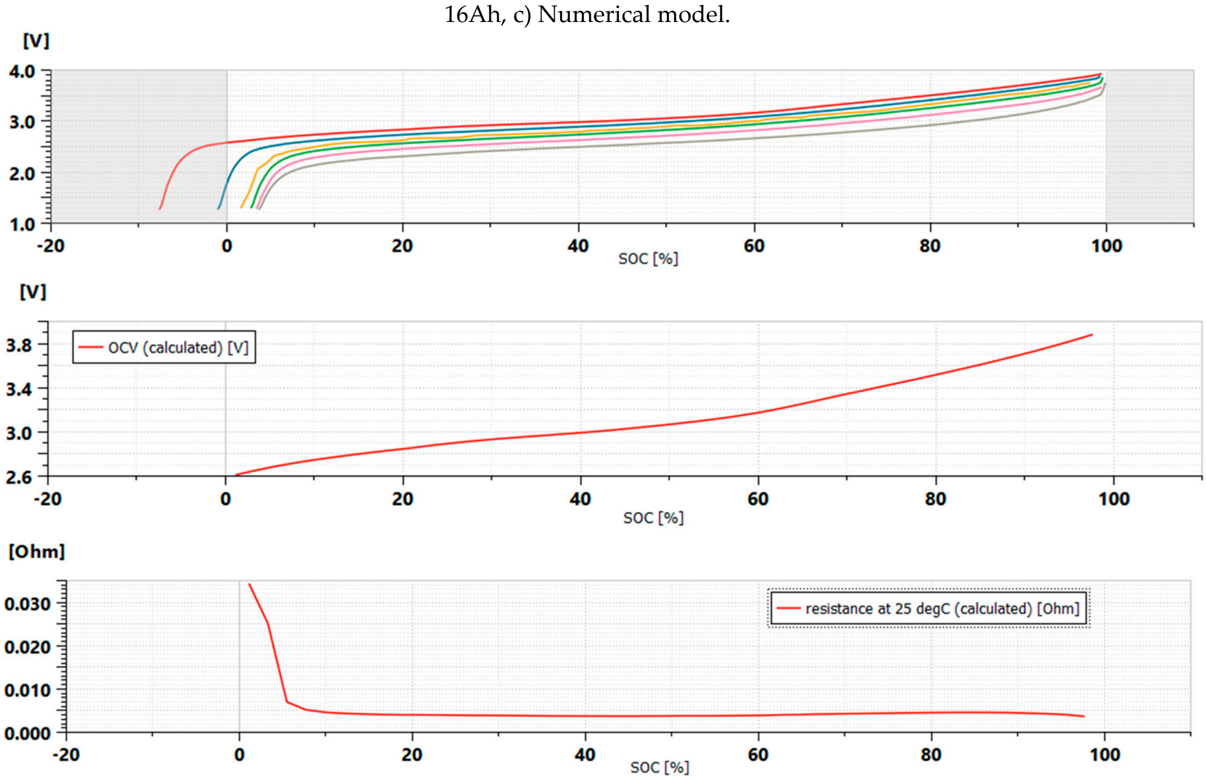

Figure 8. OCV and the resistance at 25°C at the variation of state of charge.

Preprints (www.preprints.org) | NOT PEER-REVIEWED | Posted: 30 June 2018 doi:10.20944/preprints201806.0499.v1

Peer-reviewed version available at *Aerospace* **2018**, *5*, 105; doi:10.3390/aerospace5040105

4. Study of the battery pack

The entire model of the hybrid system has been already presented (figure 4). In this section of the paper, it has been run the numerical model in order to verify the battery pack choice. For this reason, simulation have been run for both mission profiles considering the weight constrain (55-60 kg). A first test called "test 1" has been run with the training mission profile doing from 3 to 5 touch-and-go cycles. The second test, called "test 2", instead, is referred to the cruise mission profile.

4.1 Test 1: Training Profile

The first test is the "Test 1" where the numerical model has been run considering the performance requested during the training profile and listed in table 3. Table 8 summarizes all the information of the chosen battery pack. The cell used is, as said, are the Kokam 16 Ah with the total weight is of 53.6 kg. With this solution, three touch-and-go are guaranteed. First model results are shown in figure 9 a) where the temperature trend as function of the altitude and the battery heat exchange are represented. In the figure 9 b), the maximum heat exchange is relative to the phases in which the maximum electric power is required (Climb segment of the training profile). Figure 9 c) shows the voltage and current trends of the battery.

Table 8. Training profile characteristics

Training Profile	
Battery type	16 Ah
N_° cells in series	66
N_° branches in parallel	2
Total cells	132
Cell weight	0.406 kg
Total weight	53.6kg
SoC @ end	38.3%
Simulation time	1770 s
N_° cycles	3

a)

b)

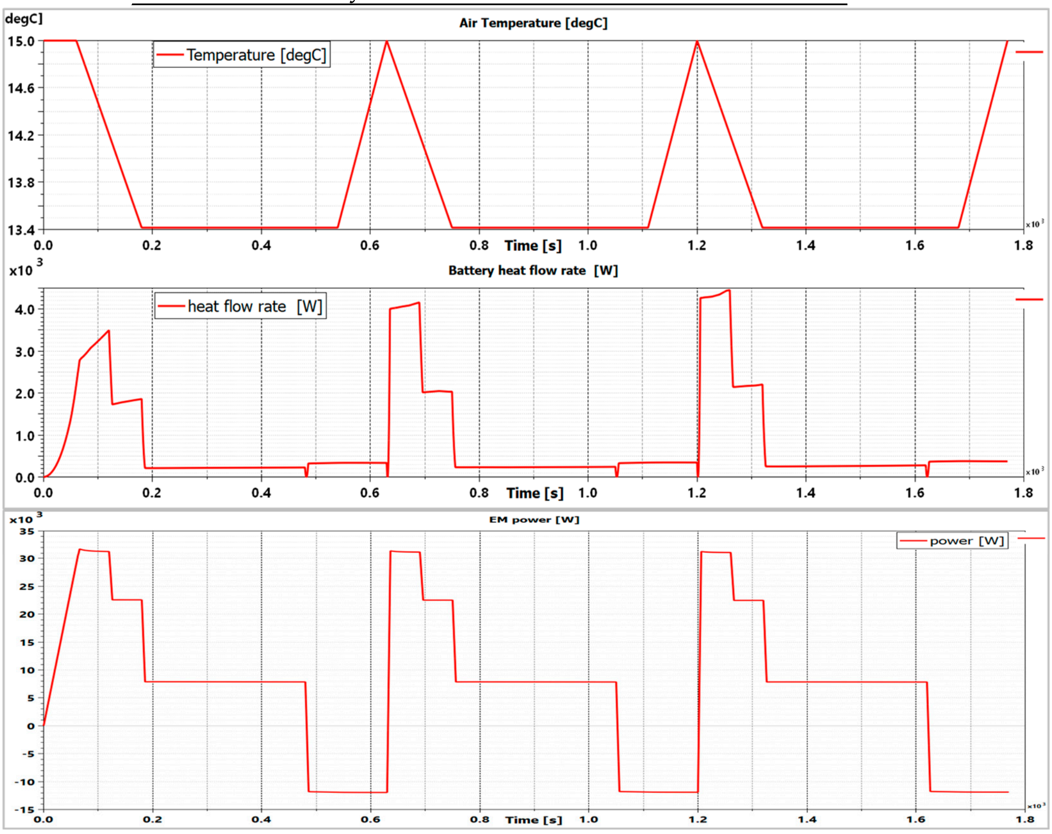

Preprints (www.preprints.org) | NOT PEER-REVIEWED | Posted: 30 June 2018 doi:10.20944/preprints201806.0499.v1

Peer-reviewed version available at Aerospace 2018, 5, 105; doi:10.3390/aerospace5040105

c)

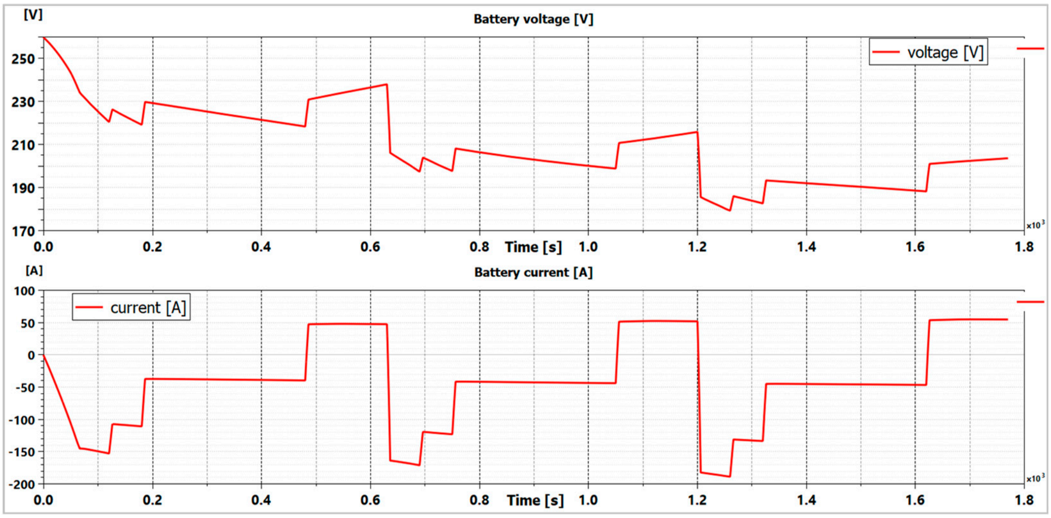

Figure 9. (**a**) Air temperature vs Battery heat flow rate, (**b**) Electric machine power, (**c**) Battery voltage and current – Training profile.

Analyzing data in figure 9, it is clear that the voltage tends decreases with the time while the current tends increases as consequence; this is true for all the phases. It is important to understand that, in the figure 9 c), the current is negative when the battery is powering the motor, while it is positive when the electric machine works as generator and recharges the battery.

By the end, another important output of the numerical model is shown in figure 10. The graph presents the state of charge of the battery pack in the training profile as function of the electric power required during the simulation time.

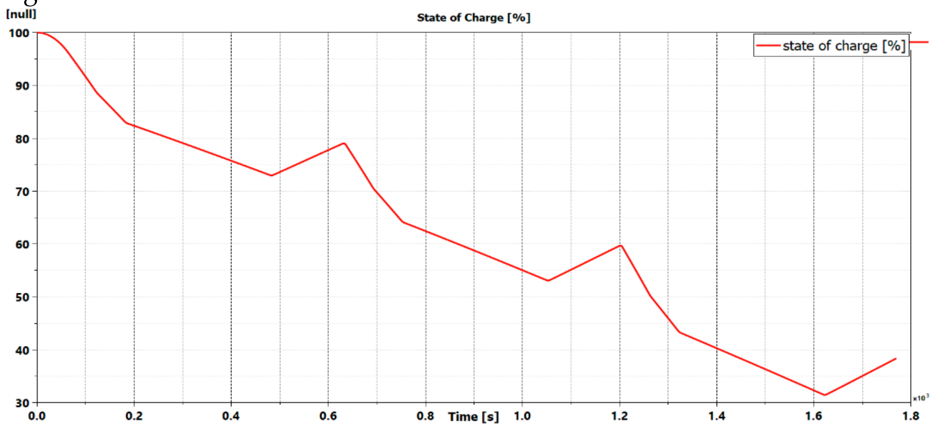

Figure 10. State of charge of the battery pack – Training profile.

Looking at the figure 10, it is clear that the system works in a fully electric configuration during the taxi phase (1 minute), in fact the slope of the curve is greater in the first phase. The electric machine, as said, works also as generator; in these phases the battery's state of charge increases. By the end, after 3 cycles, the battery still has 38.3% of charge. Even if the battery has a state of charge close to 40% at the end of the third cycle, this percentage is too low to allow the fourth cycles.

It is important to underline that the chosen battery pack configuration respects the weight limits, guarantees the power demand, and respects the actual standards on maximum voltage and the security between two branches in parallel.

4.2 Test 2: Cruise Profile

The project expected the simulation of two different mission profiles. After representing the possible configurations for the training profile; by following the numerical results obtained during the simulation in the cruise profile have been reported. The boundary conditions set in the model for the cruise mission profile are the same of table 7 except for the number of cycles (in the cruise profile consist of a single cycle).

Looking at figure 11a) the SoC at the end of the profile mission is of 47% (the overall simulation time is of 9960 s). The chosen battery pack is able to guarantee this flight profile (of 9960 s) ensuring a final cycle level of SoC of 47%. The power demand is also perfectly guaranteed as shown in figure 11). Hence, the choice of the Superior Lithium Polymer Battery SLPB78205130H of KOKAM has been numerically demonstrated to be good for both mission profiles, allowing also three touch-and-go for the training one. As said, state of charge at the end of the cruise mission profile is of 47%. This can be justified looking at the lower peak of the trend in the figure 11 a) where after the taking-off and the climb phases. At that time, the state of charge of the battery is of around 5-8%. Then, thanks to the cruise mission phase, the electric machine works as generator and consequently the state of charge increases and goes until the 47%.

a)
b)
c)

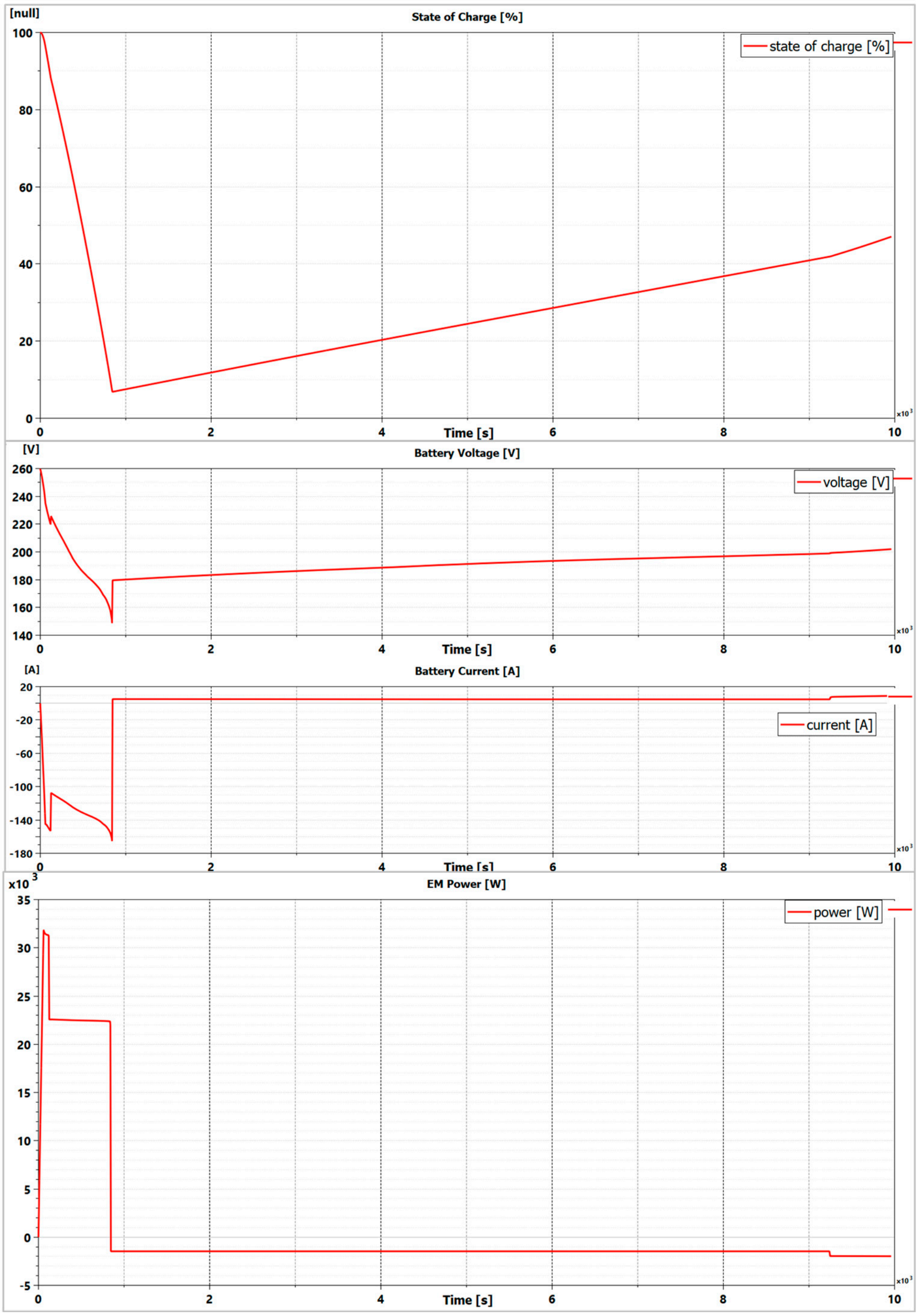

Figure 11. (**a**) The state of charge, (**b**) The battery voltage and current, (**c**) The electric machine power – Cruise profile.

The numerical model has been used, as demonstrated in this paper section, to be a good methodology to approach at the choice of a new component in the hybrid-propulsion system. In the following paragraph the numerical methodology has been adopted in order to investigate on the real improvement on the environmental emissions achieved with hybrid-electric solution.

5. Numerical model results

The numerical model described in the previous paragraph has been run following both mission profiles to evaluate the overall performance of the hybrid propulsion system.

A. Model results: Training Profile

The entire numerical model shows in figure 4 has been run for three consequent cycles. However, since the trend of the magnitudes are the same for each graft in the following figures only one cycle has been reported. Figures 12 a) and b) represent the power and rotary speed of the internal combustion engine ICE (red) and the electric machine EM (green) as function of the simulation time for one cycle.

In the figure 12 a), the powers comparison shows that the line green, related to the electric machine, becomes negative when it works as generator. In figure 12 b) represents the speed of both motors and the propeller speed, that is, as said, half of the motor speed.

The overall efficiency of the engine depends on the efficiencies of the; combustion, mechanical and thermodynamic cycle.

These parameters are function of the power loss due to the combustion, the exhaust and the mechanical components. In figure 13 these powers are represented.

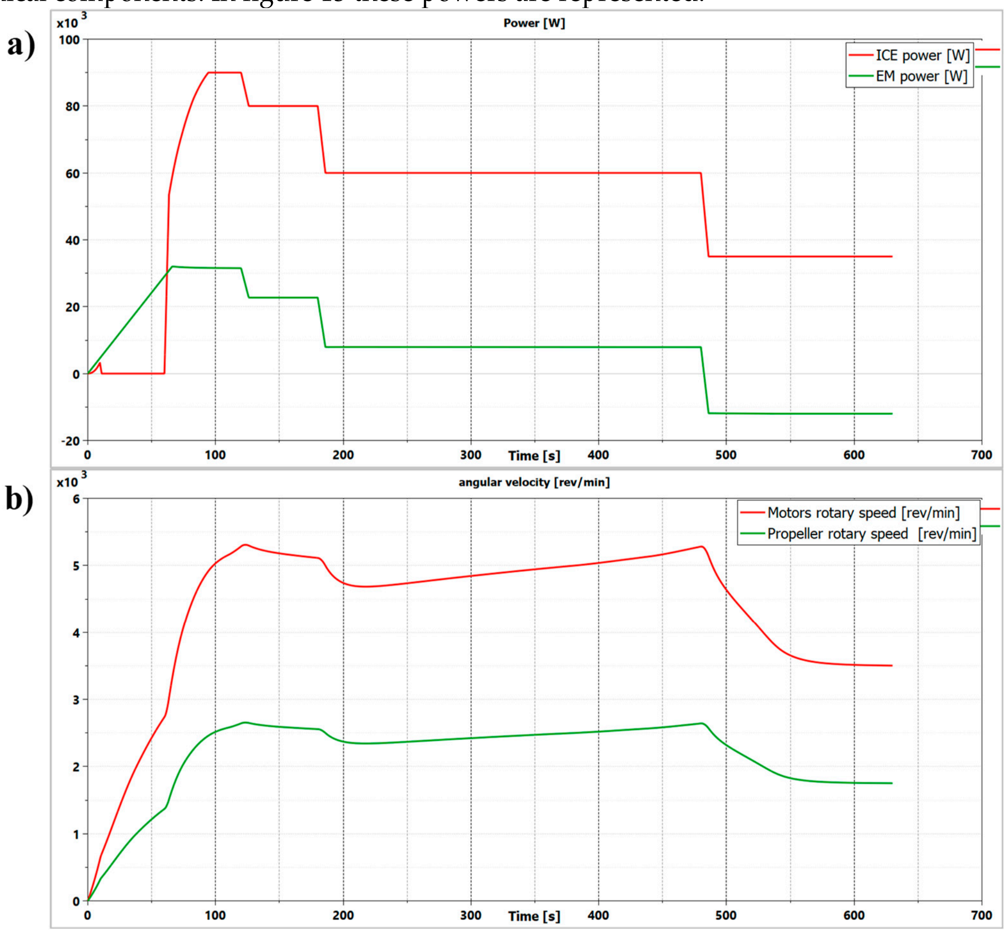

Figure 12. (**a**) ICE power and EM power, (**b**) Motor speed vs Propeller speed (Training).

Considering a maximum power of 122 kW at 100 s, the table 9 presents the values of the fuel power, exhausts power, friction power losses and mechanical power. These values allow calculating the efficiencies at maximum mechanical power. The engine performance relative to the maximum mechanical power are instead show in table 10.

Preprints (www.preprints.org) | NOT PEER-REVIEWED | Posted: 30 June 2018 doi:10.20944/preprints201806.0499.v1

Peer-reviewed version available at Aerospace 2018, 5, 105; doi:10.3390/aerospace5040105

Table 9. Power Type at Propeller (Training)

Power Type at the Max-Power at Propeller	[kW]
Fuel Power	324
Exhausts Power	106.8
Friction losses Power	13.9
Mechanical Power	122

Table 10. Performance @ Max-Power before Gearbox (Training)

Performance at the Max-Power before Gearbox (2:1) Hybrid: CMD22 + EMRAX208	
Mechanical Power [kW]	122
Torque [Nm]	230.67
Engine speed [rpm]	5053
Specific consumption [g/kWh]	293.21
Global Efficiency [-]	0.27
BMEP [bar]	9.75
IMEP [bar]	11.28

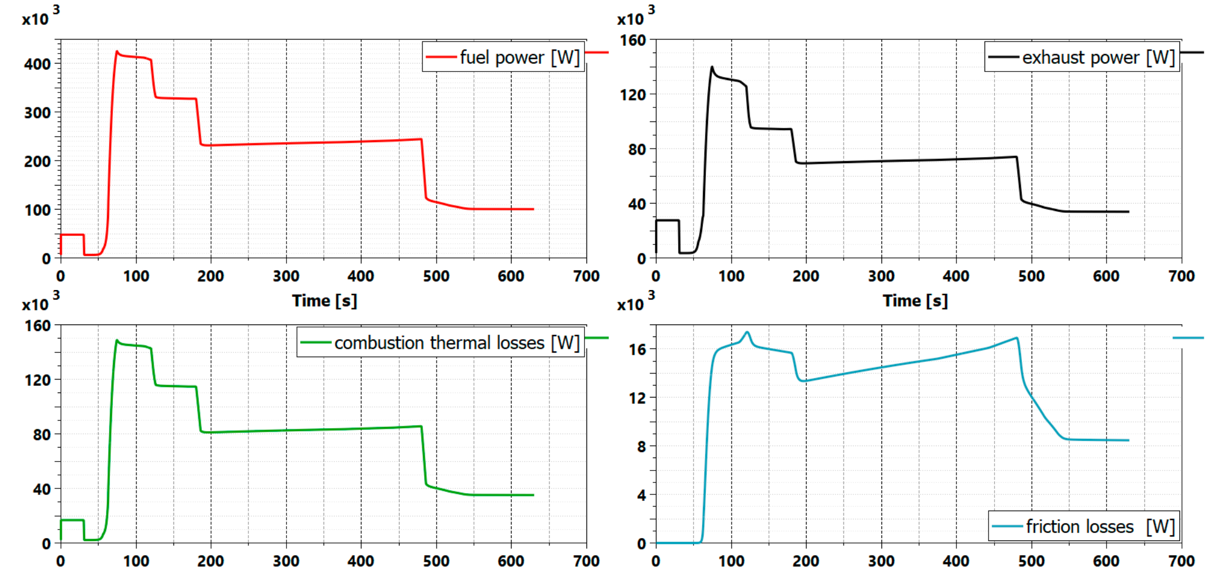

Figure 13. CMD22 power losses (Training).

5.1 Model results: Cruise Profile

At the same way, the cruise profile has been deeply investigated. Model results related to power, torque, engine speed, specific consumption, pressure, efficiency, power losses and relative efficiencies, relative to the cruise profile, have been reported in the figures below.

Also for the cruise mission profile, considering a maximum power of 122 kW the fuel power, the exhausts power, the friction of losses power and the mechanical power at 100 s are listed in table 11. Instead, in table 12 the engine performance relative to the maximum mechanical power in a determinate time instant are presented.

Peer-reviewed version available at *Aerospace* **2018**, *5*, 105; doi:10.3390/aerospace5040105

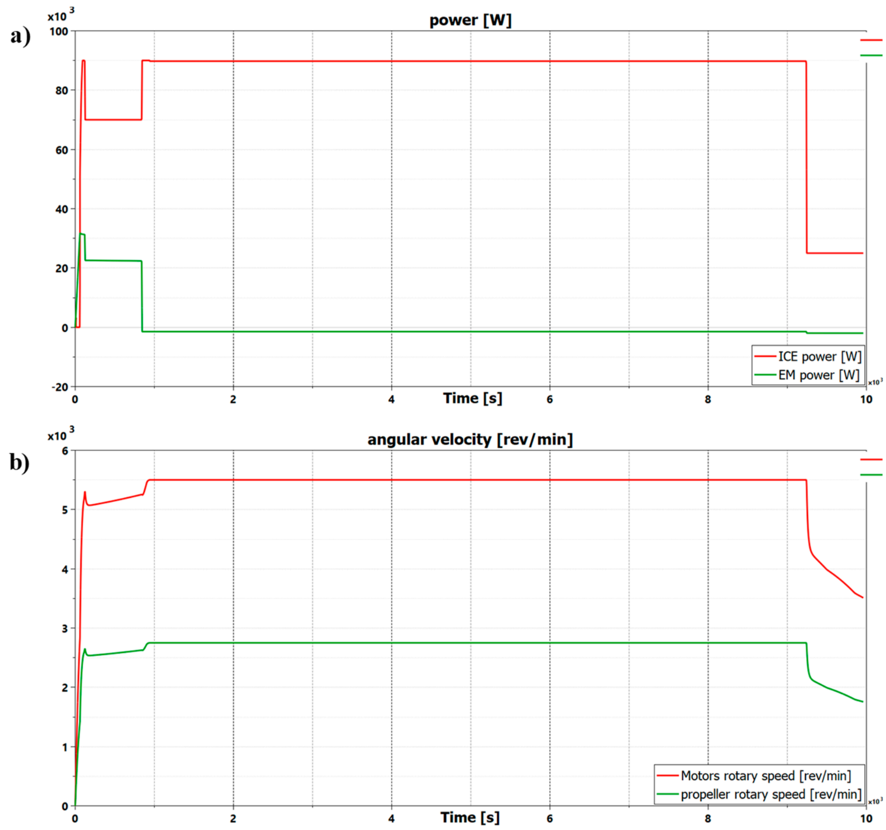

Figure 14. (**a**) Mechanical power of ICE and EM, (**b**) Motors speed vs Propeller speed – Cruise.

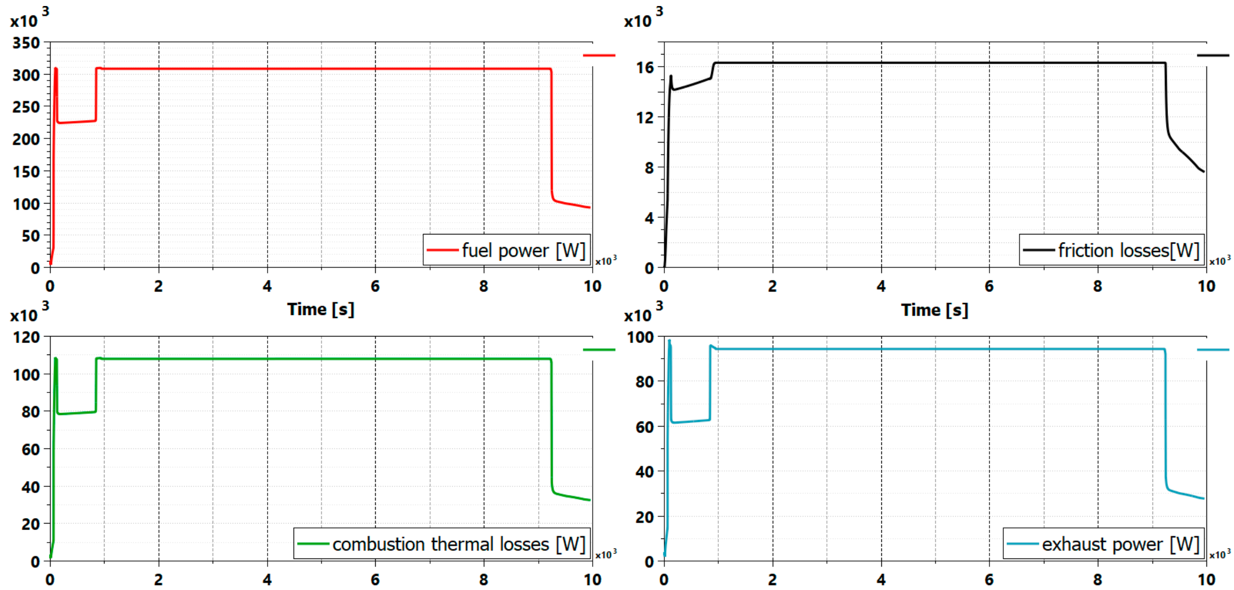

Figure 15. CMD22 power losses.

Table 11. Power Type @ Max-Power at Propeller (Cruise)

Power Type at the Max-Power at Propeller	[kW]
Fuel Power	307
Exhausts Power	95.8
Friction losses Power	13.9
Mechanical Power	122

Preprints (www.preprints.org) | NOT PEER-REVIEWED | Posted: 30 June 2018 doi:10.20944/preprints201806.0499.v1

Peer-reviewed version available at *Aerospace* **2018**, *5*, 105; doi:10.3390/aerospace5040105

Table 12. Performance @ Max-Power before Gearbox (Cruise)

Performance at the Max-Power before Gearbox (2:1) - Hybrid: CMD22 + EMRAX208	
Mechanical Power [kW]	122
Torque [Nm]	206.2
Specific consumption [g/kWh]	292.89
Global Efficiency [-]	0.29
BMEP [bar]	9.71
IMEP [bar]	11.23

6. Comparison between "baseline" and "hybrid" configurations

The numerical results obtained by running simulations on the Hybrid-Electric propulsion solution have verified that the designed system is able to perform both mission profile, respecting the weight limits. In this section of the paper the "Hybrid" and the "baseline" configuration of the propulsion system is shown [11].

In order to perform the comparison, a model of the internal combustion engine Lycoming IO-360 (baseline propulsion system) has been built up. The model of the baseline configuration is shown in figure 16.

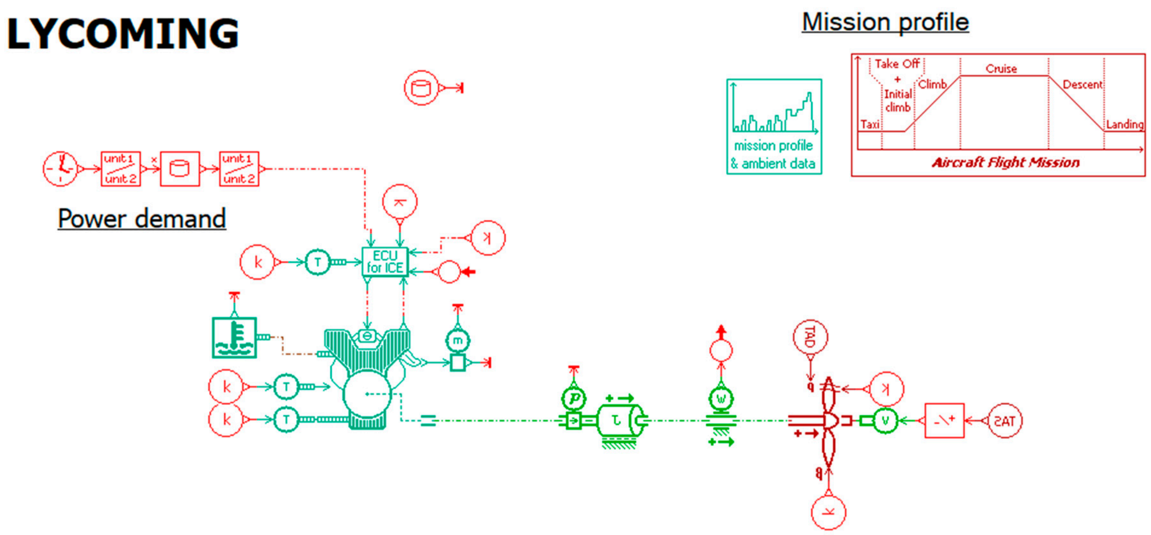

Figure 16. Model of the actual propulsion system (Lycoming IO-360).

The model architecture is similar to the hybrid system; however, in this case, engine and the propeller are connected on the same shaft, without speed reducer. The management and the model inputs are the same already explained. The significant differences between models concern the engine geometry and consequently the input to the model (figure 17).

Preprints (www.preprints.org) | NOT PEER-REVIEWED | Posted: 30 June 2018 doi:10.20944/preprints201806.0499.v1

Peer-reviewed version available at *Aerospace* **2018**, *5*, 105; doi:10.3390/aerospace5040105

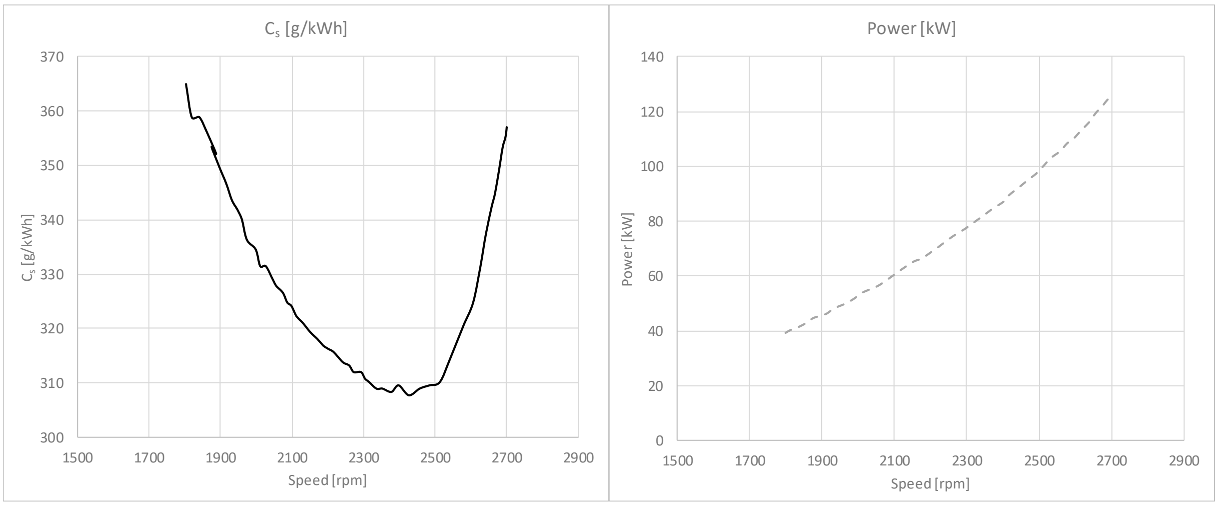

Figure 17. Lycoming Performances (Cs - Power vs engine speed).

As said, in this paragraph the comparison between the "baseline" and "hybrid" configurations has been done on the power, the speed, the torque and on the fuel saving and the CO2 emitted into the environment. The comparison between the propulsion configurations has been performed for both mission profile.

6.1 Training profile: Performance and consumption

Both model configurations have been run in the training mission profile. Figure 18 represents the trends of the power, the torque and rotary speed; that, for the hybrid configuration, have been read before the speed reducer. In figure 18, the "baseline" configuration is in red and the "hybrid" one is in black.

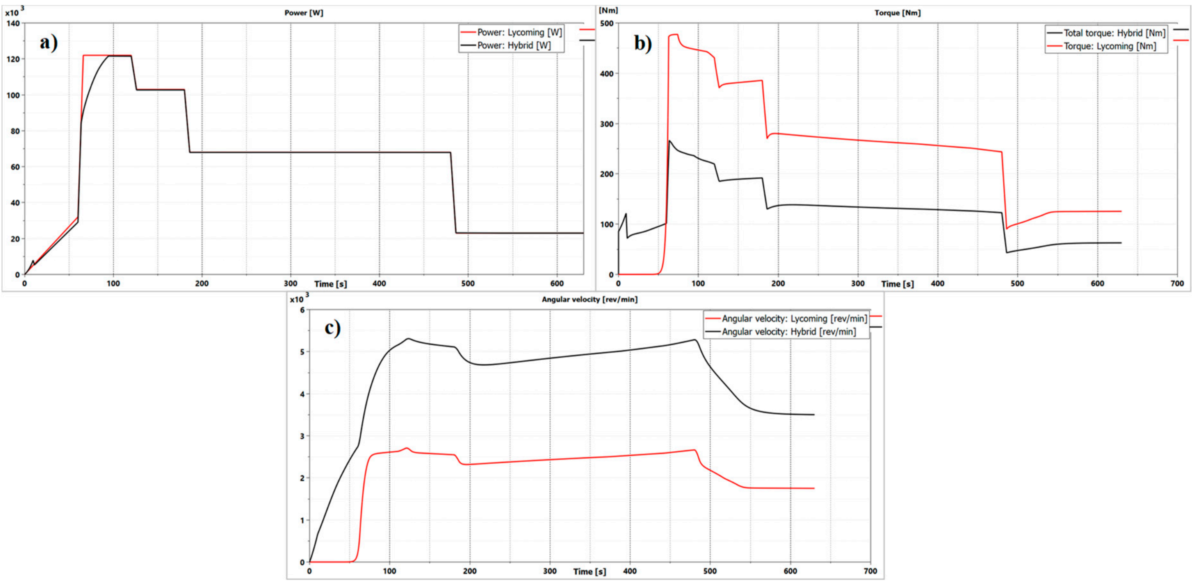

Figure 18. Comparison between configurations: (**a**) Power, (**b**) Torque and (**c**) Speeds (Training profile).

Power profiles in figure 18 a) are the same, while the torque of the hybrid configuration is one half of the other, vice versa for the rotary speed, figure 18 b) and 18c) respectively. After the speed reducer applied on the hybrid configuration, torques and speeds become equal to the baseline configuration.

Figure 19 represents the comparison between the powers used to define efficiencies. In fact, the engine efficiency depends by the combustion efficiency, the mechanical efficiency and the thermodynamic efficiency. These parameters are function of the power loss due to the combustion, the exhaust and the mechanical components.

The baseline configuration, as said, has a bigger engine with higher nominal power able to cover the power demand by itself. Otherwise, the ICE of the hybrid system is smaller and with less nominal

Preprints (www.preprints.org) | NOT PEER-REVIEWED | Posted: 30 June 2018 doi:10.20944/preprints201806.0499.v1

Peer-reviewed version available at *Aerospace* **2018**, *5*, 105; doi:10.3390/aerospace5040105

power, so it is used to cover only a part of the power demand, depending by the missions and consequently by the segments analyzed. For these reasons, trends of the powers relative to the baseline configurations are higher than the hybrid configuration.

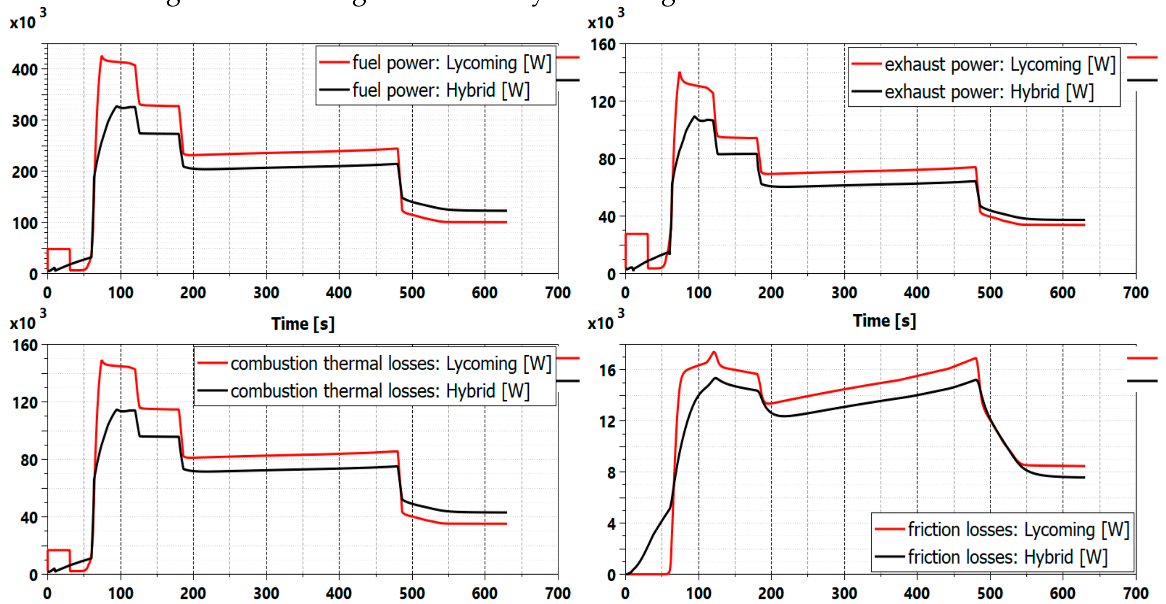

Figure 19. Comparison between the powers (Training profile).

Figure 20 a) represents comparison on the fuel consumption during the first cycle of the mission profile. However, differences between configurations has been found also for the other cycles (3-5). Other important data are shown in figure 18 b) where the comparison of the emission of CO_2 have been diagrammed.

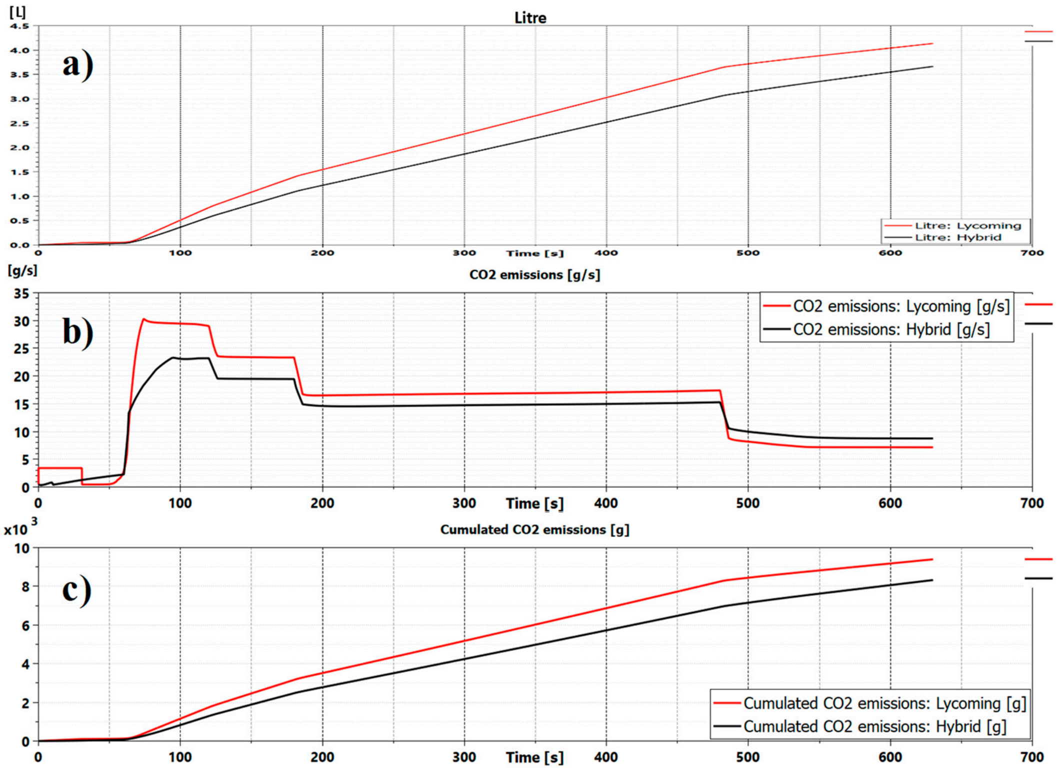

Figure 20. (**a**) Fuel consumption, (**b**) CO_2 emissions [g/s], (**c**) CO_2 cumulated [g] (Training profile).

Table 13 summarizes the numerical results showed in the previous figures. Therefore, the table reposts the consumption and emissions of the two configurations for the training profile.

 doi:10.20944/preprints201806.0499.v1

Peer-reviewed version available at Aerospace 2018, 5, 105; doi:10.3390/aerospace5040105

Table 13. Consumption and emissions (Training)

Type	Lycoming IO-360			Hybrid: CMD22 + EMRAX 208		
	1 Cycle	3 Cycles	5 Cycles	1 Cycle	3 Cycles	5 Cycles
Consumption [l]	4.33	12.55	20.95	3.66	11	18.33
Grams	3158.7	9085.1	15140.5	2641.9	7930.9	13219.8
Emitted CO_2 [g]	9950	28618.2	47692.7	8322.1	24982.5	41642.5

Tables (14 and 15), otherwise, represent the saving in terms of consumption and CO2 emission passing from the baseline configuration to the hybrid configuration for the training mission profile.

Table 14. Delta consumption (Training)

	1 Cycle	3 Cycles	5 Cycles
Liters	-0.67	-1.55	-2.62
Grams	-516.8	-1154.2	-1920.7
CO_2 [g]	-1627.9	-3635.7	-6050.2

Table 15. Percentage saving (Training)

	1 Cycle	3 Cycles	5 Cycles
Liters	15.7 %	12.4 %	12.5 %
Grams	16.4 %	12.7 %	12.7 %
CO_2 [g]	16.4 %	12.7 %	12.7 %

6.2 Cruise profile: performance and consumption

As already done for the training mission profile, models of both configurations have been run following the cruise mission profile. The values and the trends, as expected, change but the concepts expressed above about power, torque and speed are the same also for this mission profile (figure 21). The comparison has been performed also on the fuel power, exhausts power, combustion thermal losses and the friction losses, as shown in figure 22.

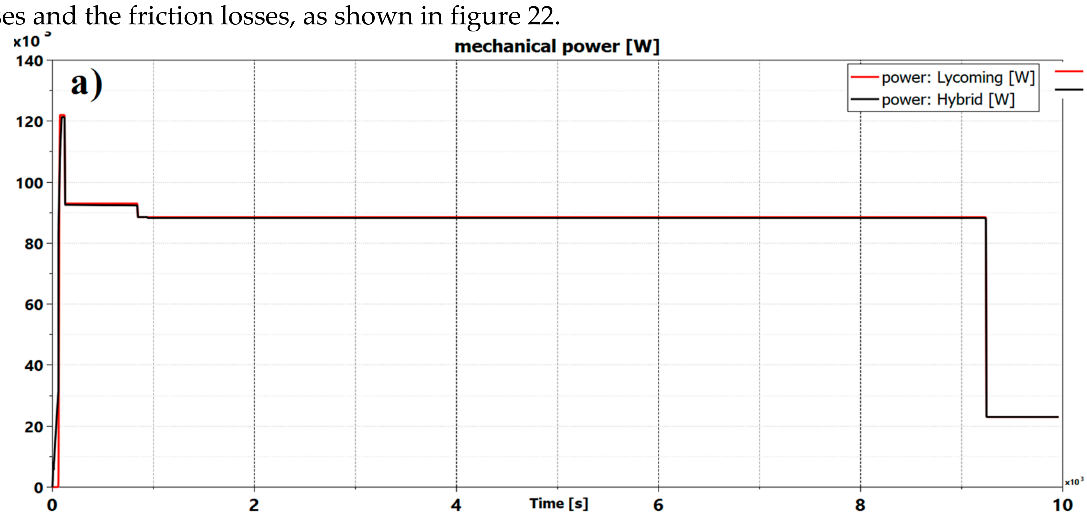

 doi:10.20944/preprints201806.0499.v1

Peer-reviewed version available at *Aerospace* **2018**, *5*, 105; doi:10.3390/aerospace5040105

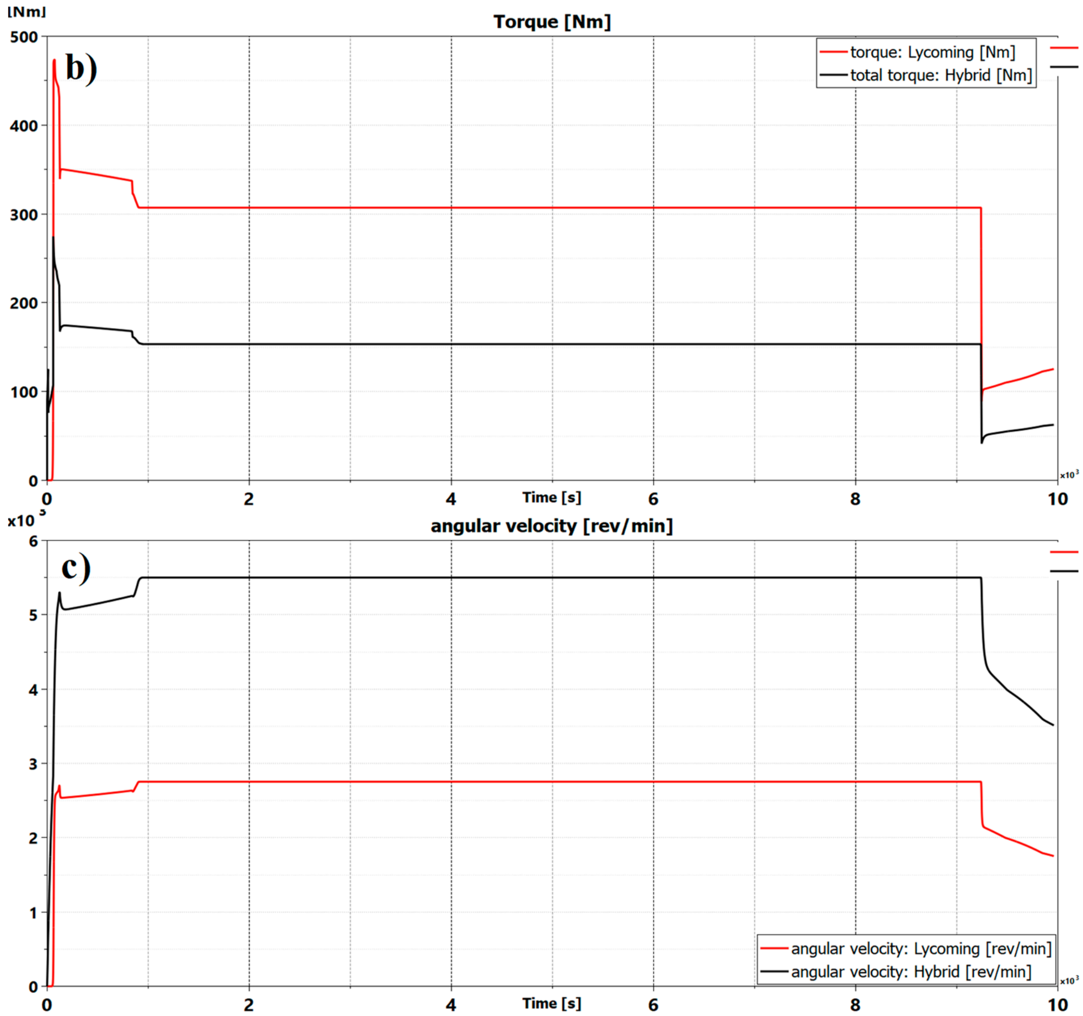

Figure 21. Comparison between configurations: (**a**) Power, (**b**) Torque and (**c**) Speeds (Cruise profile).

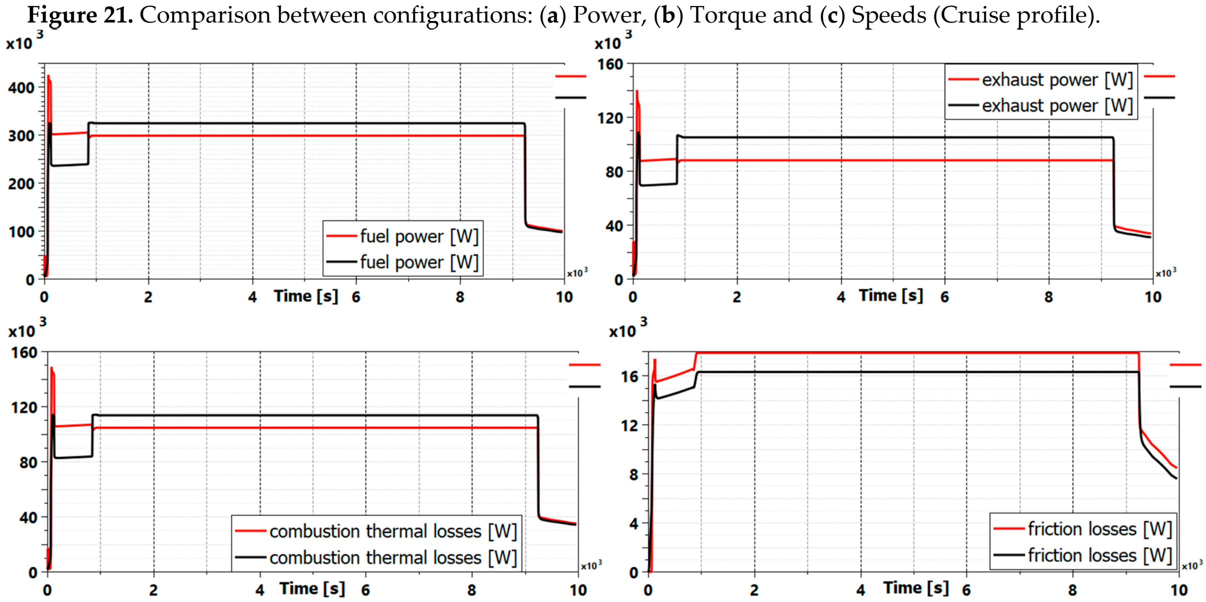

Figure 22. Comparison between the powers (Cruise profile).

Preprints (www.preprints.org) | NOT PEER-REVIEWED | Posted: 30 June 2018 doi:10.20944/preprints201806.0499.v1

Peer-reviewed version available at *Aerospace* **2018**, *5*, 105; doi:10.3390/aerospace5040105

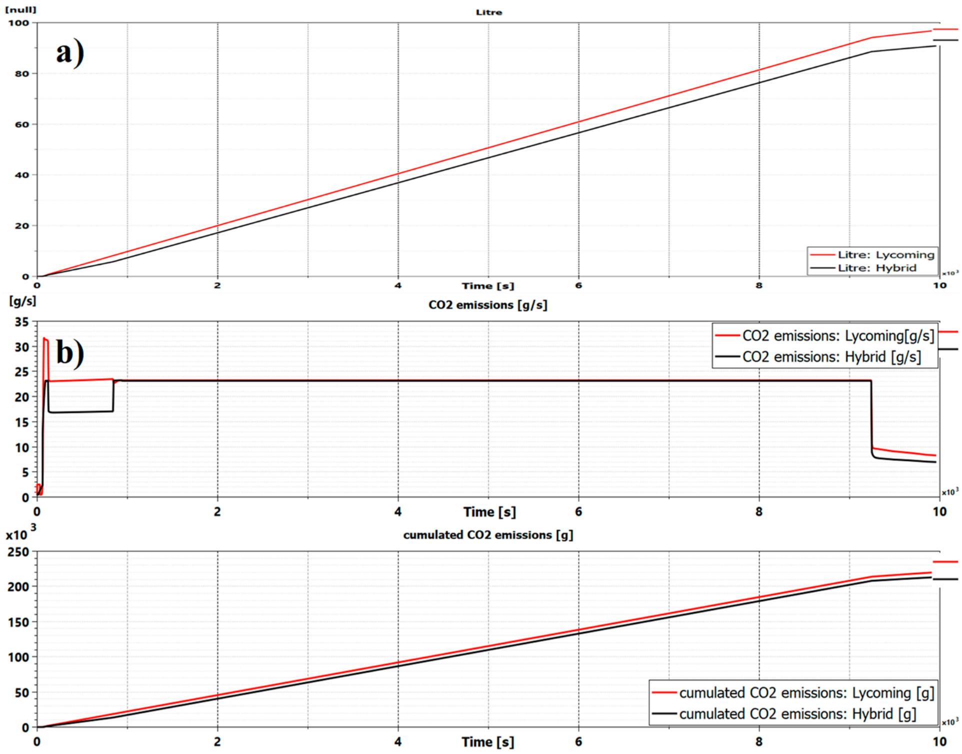

Figure 23. (**a**) Fuel consumption, (**b**) CO_2 consumption (Cruise profile).

Figure 23 shows the fuel saving also for the cruise profile confirming that also for the cruise mission profile there is a reduction of consumption ad emissions. Therefore, the goal of this research has been achieved.

The tables (16 and 17) represent the amount of saving and consequently the percentage of reduction for the cruise profile.

Table 16. Consumption and emissions (Cruise profile)

	Lycoming IO-360	Hybrid: CMD22 + EMRAX 208
Consumption [L]	96.92	90.83
Grams	69882.6	67671.5
Emitted CO_2 [g]	220130	213165

Table 17. Delta consumption and percentage saving (Cruise profile)

Delta Consumption		Percentage Saving	
Consumption [L]	-6.09	Liters	6.3%
Grams	-2211.1	Grams	3.16%
Emitted CO_2 [g]	-6965	CO_2 [g]	3.16%

Conclusions

The feasibility and the potential environmental benefits of a hybrid electric propulsion system for light aircraft has been investigated.

The paper presents an analysis of a parallel hybrid-electric propulsion system for the general aviation aircraft.

This system has been modeled with a multi-physical and multi-domain commercial code AMESim®. Each component of the system has been characterized: internal combustion engine, electric machine, mission profiles (training and cruise), battery pack, system inertia, propeller, the power demands and the flight speed.

The numerical model has demonstrated to be a useful tool for the choice and the sizing of system components. In particular, different battery configurations were examined, both with training and cruise mission profiles, giving clear indications on the best configuration of the system.

The comparison between the benchmark propulsion system -with only the ICE- and the hybrid-electric system has been the conclusive part of simulations to validate the tool. Results has shown that the hybrid-electric propulsion system for a light aircraft is advantageous for the fuel saving and the pollutants emissions decreasing. In particular, the simulations highlight a fuel saving over the 12% for the training profile and amount the 6% for the cruise profile.

All achieved results are relative to a system modeled using off the shelf component and technologies which suggests that already nowadays can be convenient operate with an aircraft powered by an hybrid-electric propulsive system.

Author Contributions: E. Frosina, G. Di Lorenzo and L. Palumbo; Methodology and Software; C. Pascarella and A. Senatore; Formal Analysis, Resources and Supervision; E. Frosina, G. Di Lorenzo and L. Palumbo; Writing-Original Draft Preparation, C. Pascarella and A. Senatore; Writing-Review & Editing.

Funding: This research received no external funding.

Acknowledgments: This research was supported by the Centro Italiano Ricerche Aerospaziali (CIRA), the company CMD and the Department of Industrial Engineering of the University of Naples “Federico II”. Authors appreciate the technical support of the companies: BSim srl and Costruzioni Aeronautiche TECNAM S.r.l.

Conflicts of Interest: The authors declare no conflict of interest.

References

1. https://www.aerospace-technology.com/projects/e-fan-electric-aircraft/
2. https://news.nationalgeographic.com/energy/2015/04/150409-epa-aviation-emissions-rules-for-airplanes/
3. https://www.britishairways.com/cms/global/pdfs/csr/CSR_web_LAQ_1_pdf_07_KMM.pdf
4. M. Cui, T. Drake, A. Kreuter, G. Kutil, B. Miller, C. Packard, M. Rahimpour e G. Soin “SOLSTICE: Standalone-electric Optimized Lifting System, Transitional Internal Combustion Engine”, Conference: 50th AIAA Aerospace Sciences Meeting including the New Horizons Forum and Aerospace Exposition, At Nashville, Tennessee, 2012, AIAA 2012-0147. doi:10.2514/6.2012-147
5. J. K. Ausserer and F. G. Harmon “Integration, Validation, and Testing of a Hybrid-Electric Propulsion System for a Small Remotely-Piloted Aircraft”, 10th International Energy Conversion Engineering Conference, International Energy Conversion Engineering Conference (IECEC), 2012. doi:10.2514/6.2012-4239.
6. C. Friedrich e P.A. Robertson “Hybrid-Electric Propulsion for Aircraft”, *AIAA Journal of Aircraft*, Vol. 52, No.1, 2015, pp. 176-189. doi: 10.2514/1.C032660.
7. Tecnam P2010 - https://www.tecnam.com/aircraft/p2010/
8. https://www.lycoming.com/content/operator%27s-manual-%28L%29IO-360-M1A-60297-36
9. CMD 22 engine - http://cmdavio.com/cmd22-aircraft-engine/
10. EM Emrax 208 - http://emrax.com/products/emrax-208/
11. Frosina, C. Caputo, G. Marinaro, A. Senatore, C. Pascarella, G. Di Lorenzo, “Modelling of a Hybrid-Electric Light Aircraft”, *Energy Procedia*, Vol. 126, (2017), pp. 1155-1162. doi: 10.1016/j.egypro.2017.08.315.
12. P.J. Masson, A. Luongo, “High Power Density Superconducting Motor for All-Electric Aircraft Propulsion”, *IEEE Transactions on Applied Superconductivity*, Vol. 15, No. 2, (2005), pp. 2226 – 2229 doi: 10.1109/TASC.2005.849618
13. P. J. Masson, D. S. Soban, E. Upton, J. E. Pienkos, and C. A. Luongo, “HTS Motors in Aircraft Propulsion: Design Considerations”, *IEEE Transactions on Applied Superconductivity*, Vol. 15, No.2, (2005), pp.2218 - 2221. doi: 10.1109/TASC.2005.849616
14. https://www.plm.automation.siemens.com/it/products/lms/imagine-lab/amesim/

Peer-reviewed version available at *Aerospace* **2018**, *5*, 105; doi:10.3390/aerospace5040105

15. J.C. Álvarez Antón, P.J. García Nieto, F.J. de Cos Juez, F. Sánchez Lasheras, M. González Vega, M.N. Roqueñí Gutiérrez, Battery state-of-charge estimator using the SVM technique", *Applied Mathematical Modelling*, Vol. 37, (2013), pp. 6244-6523. doi: 10.1016/j.apm.2013.01.024
16. X. Zhang, W. He, Y. Zhang, M. D.Pandey, An effective approach for probabilistic lifetime modelling based on the principle of maximum entropy with fractional moments, *Applied Mathematical Modelling*, Vol. 51, (2017), pp. 626-642.